Doc Ophthalmol (2026) 152:287–307
https://doi.org/10.1007/s10633-026-10093-y

REVIEW ARTICLE

Review of the clinical electrooculogram - Part 2: the bestrophinopathies and modified protocols

Srikanta Kumar Padhy · **Maja Šuštar Habjan** · **Paul A. Constable**

Received: 21 August 2025 / Accepted: 17 February 2026 / Published online: 8 March 2026

Abstract The light-rise of the electro-oculogram (EOG) is used as a clinical marker for a collection of disorders known as the 'bestrophinopathies.' This review provides an overview of these conditions including Best Vitelliform Macular Dystrophy (BVMD, Autosomal Recessive Bestrophinopathy (ARB), Adult Onset Vitelliform Macular Dystrophy (AVMD) and Autosomal Dominant Vitreoretinal-choriodopathy (ADVIRC) and potential future therapies. One drawback of the EOG is the time to administer the test and shortened protocols that have been developed to improve the clinical testing of the EOG which include incorporating measures during recordings of the ERG or shortening the period of dark and light adaptation. The companion paper summarizes the cellular mechanism of the EOG, and this review is focused on the clinical applications of the EOG.

Keywords Bestrophin · Light-rise · Retinal pigment epithelium · Protocol · Standing potential · Maculopathy

Supplementary Information The online version contains supplementary material available at https://doi.org/10.1007/s10633-026-10093-y.

S. K. Padhy
Anant Bajaj Retina Institute, LV Prasad Eye Institute, Mithu Tulsi Chanrai Campus, Bhubaneswar 751024, India
e-mail: srikanta.padhy@lvpei.org

M. Š. Habjan
Department of Ophthalmology, University Medical Centre Ljubljana, Grabloviceva 46, 1000 Ljubljana, Slovenia
e-mail: maja.sustar@kclj.si

P. A. Constable (✉)
College of Nursing and Health Sciences, Caring Futures Institute, Flinders University, Adelaide, Australia
e-mail: paul.constable@flinders.edu.au

Background

The clinical electrooculogram (EOG) [1] is a functional test of the retinal pigment epithelium (RPE) that supports visual processes of the outer retina [2]. The RPE forms a monolayer of cuboidal cells that are hexagonally arranged with the highest density at the fovea [3]. The apical membrane has microvilli that interdigitate with the outer segments of the rod and cone photoreceptors. The basolateral membrane is continuous with the underlying Bruch's membrane [4]. Tight junctions are formed between the RPE cells to form a selective barrier and provide electrical resistance between the apical and basolateral membrane electrical potentials [5]. The functions of the RPE are diverse including fluid regulation, light absorption, phagocytosis, ionic homeostasis, glucose transport to the photoreceptors and growth factor secretion to maintain permeability of the underlying choroid and maintain photoreceptor function [2]. The clinical EOG is helpful in conditions that affect the role of bestrophin primarily in diagnosing a collection of disorders referred to as 'the bestrophinopathies

[6, 7] arising from pathogenic variants in *BEST1* [8]. This paper focusses on the clinical aspects of the EOG whilst the accompanying companion paper explores the current mechanism of the light-rise of the EOG with particular emphasis on the role of bestrophin in regulating intracellular calcium and basolateral chloride conductance through voltage gated anoctamin channels.

The bestrophinopathies include a spectrum of retinal disorders caused by disease-causing variants in the *BEST1* gene. These include Best vitelliform macular dystrophy (BVMD), adult-onset vitelliform macular degeneration (AVMD), autosomal dominant vitreoretinochoroidopathy (ADVIRC), and autosomal recessive bestrophinopathy (ARB) [7, 9]. These conditions primarily affect the macula and are typically present within the first two decades of life. *BEST1* pathogenic variants affect trafficking and normal functioning of the L-type Ca^{2+} channel including phagocytosis [10, 11], cell volume regulation [12] further contributing to the pathophysiology of the bestrophinopathies [13, 14]. The macular vitelliform lesions that characterize BVMD may be a result of the low expression of bestrophin in this region of the eye making the central region more susceptible to pathological changes [15]. Despite its milder phenotype, AVMD remains clinically indistinguishable from early-stage BVMD in many cases. This phenotypic overlap has led to the proposal that AVMD represents either an attenuated [16] or a sub-type of BVMD [17] rather than a distinct entity. It should be noted that although *BEST1* variants are the most widely recognized cause of vitelliform lesions, adult-onset presentations are genetically heterogeneous, with *PRPH2* [18, 19], *IMPG1, IMPG2,* [20–22], *HTRA1* [23], and *CTNNA1* [24], with others also implicated. *PRPH2* being most common and *BEST1/VMD2* the second most common [18].

The EOG is typically abnormal in conditions affecting the outer retina/RPE or the choroid such as secondary to drug toxicity or ischemia. Conditions in which abnormal EOGs, characterized by a reduction in the light-rise have been reported include pigmented paravenous retinochoroidal atrophy [25], posterior multifocal placoid pigment epitheliopathy [26], pattern dystrophy [27], X-linked carriers of retinitis pigmentosa [28], membranoproliferative glomerulonephritis type II [29], gyrate atrophy [30], Helicoidal peripapillary chorioretinal degeneration [31], unilateral acute idiopathic maculopathy [32] and North Carolina Macular Dystrophy (NCMD) [33]. Whilst the main use of the EOG is in the bestrophinopathies, other clinical conditions may reveal reductions in the light-peak such as Danon's Disease with low Dark Trough (DT) and LP amplitudes [34] and bilateral optic neuropathy [35]. Vigabatrin therapy can lead to loss of visual fields and reduced EOGs secondary with a loss in RPE function [36]. The EOG may be affected in chloroquine retinopathy but is not recommended as a standard screening tool [37]. A case report following tamoxifen retinopathy has been reported with a reduced $LP:DT_{ratio}$ [38]. Most commonly the EOG is associated with a collection of disorders associated with pathogenic variants in *BEST1* [39] that result in visual loss and are associated with the accumulation of exudate in the sub retinal space [40]; with outer retinal changes associated with worse visual acuity [41]. The spectrum of phenotypes relating to BVMD, ARB and ADVIRC depend upon the pathogenic variants in *BEST1* [42]. Large phenotype-genotype descriptions have been described for BVMD in Chinese [43], Italian [44], United Kingdom [45, 46], and Danish [47] populations.

The EOG is of benefit when diagnosing conditions affecting bestrophin, the clinical test can be arduous and time-consuming in the clinic. Shortened protocols that integrate the EOG recording into the ISCEV standard ERG recording protocol have been proposed [48]. In addition, reducing the dark- and light-adapted times to 6- and 10-min intervals respectively to reduce the overall EOG test time [49]. Modifying the existing ISCEV standard test protocol [1] may help to improve the clinical utility of the EOG as a test for RPE function. For a review of the current EOG recording protocols and mechanism see the companion paper and Constable (2024) [50], Constable (2014) [51] and Arden and Constable (2006) [52].

Bestrophinopathies

Disease causing variants in *BEST1* cause mislocalization or loss of function, but the specific pathogenic variant is not related directly to the disease phenotype [11]. The compound heterozygous R141H and Y29stop pathogenic variants were identified in a Swedish family with BVMD [53] with another early report identifying a variant

in in exon 8 p.E292K with all affected individuals having reduced light-peak to dark-trough ratios ($LP:DT_{ratios}$) [54]. When BVMD disease causing variants associated with *BEST1* were explored including (V9M, W93C, and R218C) in transfected Madin-Darby Canine Kidney (MDCK) cells the expression profile revealed that the R218C variant in Best1 was basolaterally localized with the W93C and V9M Best1 variants deposited intracellularly. The authors concluded that there were likely to be at least three basolateral sorting motifs that affected the localization of bestrophin [55]. Localization has also been implicated in the following pathogenic variants following transfection in cell lines (Y85H, Q96R, L100R, Y227N and Y227E) [56], and (T6P, L21V, W24C, L224M, Y227N, T237R, F305S and V311G) also show trafficking errors with these disease causing variants on the cytoplasmic face compared to pathogenic variants in the membrane domain (S79C, F80L, L82V and A243T) [57].

Whilst no treatment is currently available, gene therapies are being explored that may prevent visual loss through the restoration of *BEST1* function [58–63]. Therapeutics targeting *BEST1* also show promise with 25 μM tadalafil restoring bestrophin function *in-vitro* [64], 4-phenylbutyrate (4PBA) also restoring function in transfected cell lines [65] and more recently in RPE cells derived from patients with dominant and recessive bestrophinopathies [66]. A natural substance, curcumin, has also increased bestrophin function and tight junctions in iPSC-RPE cells [67]. An early clinical trial using docosahexaenoic acid supplementation showed no clinical efficacy [68].

Human embryo-derived pluripotent stem cells (PSC-RPE) [69] and induced pluripotent stem cells (iPSC-RPE) [70, 71] cultures provide a new method to explore therapeutic and gene-based therapies *in-vivo* [59, 72–75]. Gain-of-Function (GOF) through gene editing has also been demonstrated in *in-vivo* with increased TMEM-16A currents [76]. Transfection in human RPE cell cultures with plasmids carrying three *BEST1* disease causing variants p.V143F, p.S142G, and p.A146T initiated apoptosis of RPE cells [70]. Successful restoration of retinal structure has been demonstrated with gene therapy in canine that holds promise for translation to humans with canine disease exhibiting similar characteristics to human BVMD [77].

Disease-causing variants in the *peripherin/RDS* gene are a recognized cause of autosomal dominant macular dystrophies, including AVMD, pattern dystrophies, and cone-rod degeneration. Most pathogenic variants are missense variants in the intradiscal D2 loop, a region essential for protein folding and ROM-1 interaction. The P210R pathogenic variant is one of the most studied, showing intrafamilial variability and a wide phenotypic spectrum from vitelliform lesions to geographic atrophy and choroidal neovascularization [78]. Detection rates vary across populations, from 7 to 23%, and frameshift variants are also reported in certain phenotypes like multifocal pattern dystrophy. Although *peripherin/RDS* is important, it accounts for only a minority of AVMD cases, highlighting the genetic heterogeneity of adult-onset macular dystrophies. Genotype–phenotype correlations suggest missense pathogenic variants may lead to severe disease, while Loss-of-Function (LOF) variants are linked to milder forms [79].

Best's vitelliform macular dystrophy

Best vitelliform macular dystrophy (BVMD) is an autosomal dominant macular dystrophy caused by pathogenic variants in *BEST1*, encoding the calcium-activated chloride channel Bestrophin-1 that is localized to the endoplasmic reticulum and basolateral membrane of the retinal pigment epithelium (RPE) [80, 81] at the basolateral RPE. It typically begins in childhood and is characterized by abnormal RPE–photoreceptor interaction and reduced EOG light-rise with a generally normal ffERG until late disease [9, 53, 82].

BVMD progresses through defined clinical stages: an early pre-vitelliform stage with subtle Optical Coherence Tomography (OCT) abnormalities and possible $LP:DT_{ratio}$ reduction; the classic vitelliform ("egg-yolk") stage with subretinal accumulation of lipofuscin-rich material; a pseudohypopyon stage where material layers inferiorly; a vitelliruptive or "scrambled-egg" stage marked by fragmentation and resorption; and a final atrophic/fibrotic stage with photoreceptor loss, macular thinning, and potential choroidal neovascularization (CNV) [45, 46]. Although this sequence is typical [40], disease severity and progression rate vary widely [9, 45, 46, 83], and atypical presentations-including unilateral

involvement [84], diabetic retinopathy [85], focal choroidal excavation [86], macular hole [87], and CNV-have been reported [88].

Early changes in BVMD affect the interdigitation between the outer segments and apical membrane of the RPE [89] and have been observed in individuals less than 10 years of age [90]. Pre-clinical investigations in six individuals with *BEST1* disease causing variants reported a decreased LP:DT_{ratio} in 5 of 12 eyes and abnormal OCT findings in three subjects with p.V9A; p.R92C; p.I230T variants characterized by heightened reflectance between the RPE and outer segments [91]. Quantitative fundus autofluorescence is reported as normal except for the intense fluorescence associated with the bullous central detachment containing lipofuscin [92] that contains increased accumulation of bis-retinoid N-retinyl-N-retinylidene ethanolamine (A2E) [93]. Reduced global chromatic and achromatic contrast sensitivity reduces with disease duration [94]. The vitelliform lesion, the hall mark of BVMD typically is described as having an 'egg-yolk' appearance of accumulated fluid and lipofuscin [95]. Imaging studies using near infrared autofluorescence may be helpful in determining the previtelliform stage [96] with 34.7% showing regions of fundus autofluorescence at the posterior pole and a reduction in central retinal thickness with age [46]. Case reports have reported unusual presentations including bilateral macular holes [97], unilaterally [82, 84], focal choroidal excavations [98], rarely a near normal LP:DT_{ratio} [99], bulls-eye maculopathy [100], peripheral retinal schisis [101], and choroidal neovascularization [88]. Clinicians should be aware that similar findings to BVMD have been reported in NCMD [33] and that, an abnormal EOG with a normal ERG, long considered characteristic of Best vitelliform macular dystrophy (BVMD), is not unique to BEST1-related disease. Small et al. (2022) [33] demonstrated that patients with NCMD can exhibit the same electrophysiologic profile, challenging the specificity of the EOG as a diagnostic marker and indicating that reduced EOG light rise may reflect localized rather than widespread RPE dysfunction. This phenotypic overlap reinforces the need for molecular confirmation and multimodal assessment, particularly in the context of patient selection for emerging *BEST1*-targeted gene therapies. See Bianco et al. (2024) [83] for a review of the clinical features of BVMD and Fig. 1.

Disease causing variants in *BEST1* include a heterozygous c.614 T > C (p.I205T) pathogenic variant in exon 5 [102], in a Chinese population novel disease-causing variants include (T2N, L75F, S144N, R255W, P297T, D301G and R218C) [103]. Dominant bestrophinopathies are predominantly associated with missense variants located in functional regions of *BEST1* with clinical features including hyperopia and glaucoma overlapping with ARB [43].

Clinical electrophysiology in BVMD typically demonstrates a reduced to absent EOG LP:DT_{ratio}—with reported values ranging from an absent light-rise to a LP:DT ratio of 3.10 [9, 18, 20, 21, 47, 53, 54, 82, 84, 85, 100, 101, 104, 105] (see Table S1 in Supplementary Material). The ffERG findings are generally normal in early disease stages under both dark- and light-adapted conditions. However, as BVMD progresses, delays in peak times and reductions in amplitudes may develop [106, 107]. Macular function assessed using mfERG demonstrates reduced amplitude in the central two rings, which correlates with the degree of subretinal fluid [47]. Polosa et al. (2025) [107] reported similar findings in adult patients. The pERG reveals reductions in p50 and n95 amplitudes when visual acuity falls below 0.5 LogMAR [106] or when photoreceptor loss occurs [108].

Autosomal dominant vitreoretinochoroidopathy

ADVIRC (Autosomal Dominant Vitreoretinochoroidopathy) is a distinct *BEST1*-associated disorder characterized by a peripheral circumferential band of retinal hyperpigmentation, which is a consistent feature across all ages [109]. The disease is typically slowly progressive, with initial preservation of central vision and visual fields, but with gradual loss of peripheral field and retinal function over time [110]. First described by Kaufman et al. (1982) [109] in a family that exhibited peripheral hyperpigmentation, cataract, high myopia with loss of retinal function in advanced stages. Mainguy et al. (2024) [110] first reported the c.1101–1 G > T splice-site pathogenic variant in *BEST1* causing ADVIRC, demonstrating altered splicing and intrafamilial phenotypic variability. The ffERG findings are generally well preserved but have been reported to range from normal to severely reduced amplitudes, that correlate with age and disease severity, based

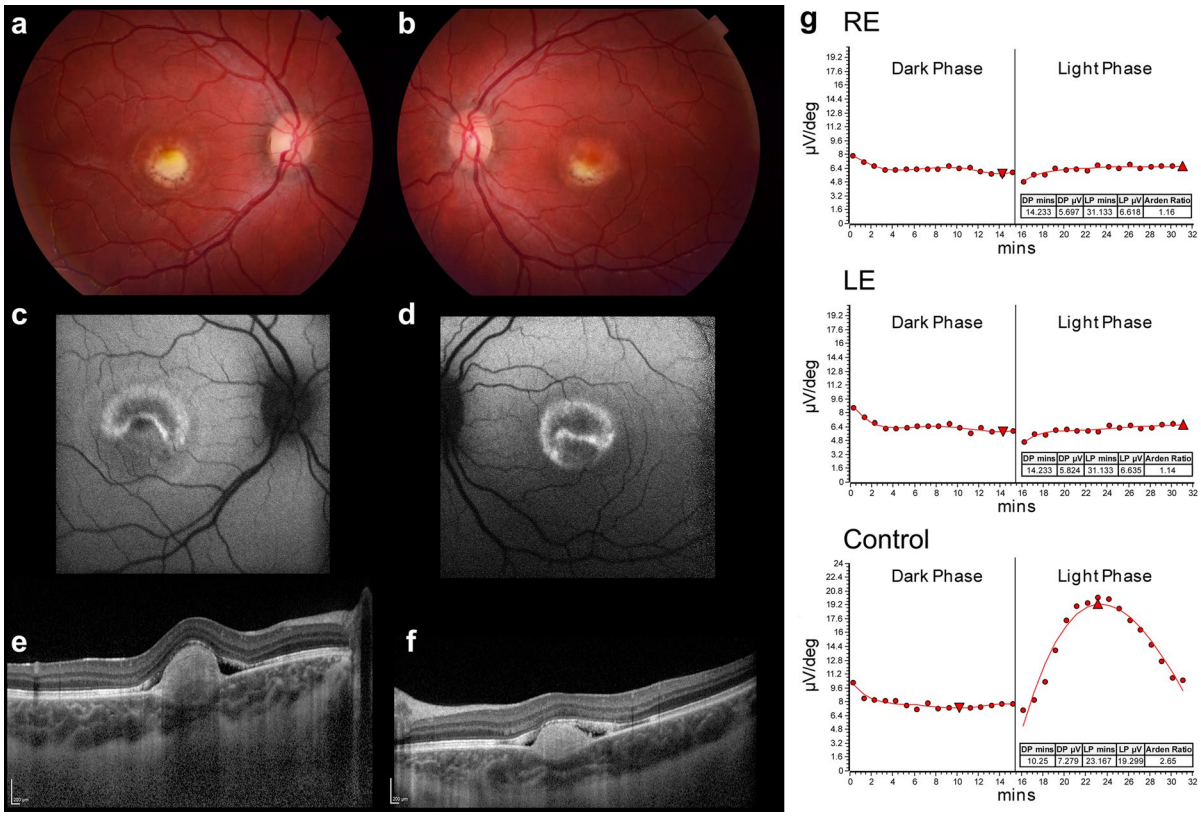

Fig. 1 Typical clinical presentation of Best Vitelliform Macular Degeneration. Color fundus photographs **(a, b)** showing central vitelliform with hyper and hypo fluorescent contents containing fluid and lipofuscin **(c, d)**. Optical Coherence Scan through the macula showing the bilateral raised central lesions **(e/f)**. Electrooculograms of the Right (RE) and Left eyes (LE) show a flat response to a change in the standing potential during the light phase. In contrast the Control electrooculogram exhibits a light-rise during the light phase with an increase in the standing potential that is dependent on normal bestrophin function within the retinal pigment epithelium

on a retrospective review of a family containing 6 members with the p.V86M variant [111]. In a novel case report of a 33-year-old female who was heterozygous for c.1101–1 G > T variant resulting in an in-frame deletion (p(S367_N579del)) and exclusion of exon 10 with reduced scotopic ffERGs and diminished light-rise and bilateral hyperpigmented and atrophic hyperpigmented peripheral retina. Of note were that her mother and half-sister who were carriers of the same disease-causing variant also exhibited fundus changes similar to the presenting case [110]. The long-term changes in ADVIRC were reported in a case after twenty-years follow-up who developed macular atrophy and unilateral hyperpigmentation with the authors suggesting that chorioretinal atrophy of the macula can occur in the later stages of ADVIRC [112].

Importantly, ADVIRC is frequently associated with developmental ocular anomalies, including microcornea, angle-closure glaucoma, and cataracts [111, 113]. Associations such as iris dysgenesis and optic nerve dysplasia have also been reported. These anomalies, along with the retinal phenotype, may result from aberrant splicing of *BEST1* transcripts, leading to internally deleted or duplicated exons [110]. The commonly reported p.V86M pathogenic variant, for instance, has been linked to such splicing defects and abnormal EOG responses, although mild or early phenotypes may occasionally show a borderline light-rise [111]. For a review of pathogenic variants associated with BVMD the reader is directed to White et al. (2000) [114].

Autosomal recessive bestrophinopathy

Autosomal recessive bestrophinopathy (ARB) commonly presents with multifocal vitelliform lesions and irregularities of the RPE, which appear as mixed areas of increased and decreased autofluorescence at the posterior pole [115]. Additional ocular findings frequently include intraretinal fluid [116], hyperopia, and, in certain individuals, shallow anterior chambers that increase the risk for angle-closure glaucoma [117]. ARB was first described by Burgess et al. (2008) [117] with a severely diminished or absent light-rise with reduced and delayed light- and dark-adapted ERGs and pattern ERGs. In a case report of a child a reduced LP:DT_{ratio} was described and mfERG reductions as well as delayed peak times for ERG, with associated RPE deposits and outer retinal changes with elongated and thickened photoreceptor outer segments, narrow anterior chambers has also been reported [118]. Modelling of ARB disease-causing variants suggest that the main reason for pathological changes is due to a lack of trafficking of bestrophin-1 [119].

Two novel pathogenic variants, c.202 T > C (chr11:61,722,628, p.Y68H) and c.867 + 97G > A, in *BEST1* have been reported in two ARB families using third generation sequencing [120]. Novel pathogenic variants also include compound heterozygous for (L40P) and (A195V) *BEST1* variant [121]. Other homozygous variants including, c.521_522del and c.1100 + 1G > A have also been reported [122]. Not all variants associated with ARB result in complete loss of function. Given the autosomal recessive inheritance pattern, a single pathogenic allele is not expected to cause disease in isolation. Accordingly, the R141H (CGC > CAC) variant alone (*Best1/Best1*^{R141H}) does not produce a clinical phenotype and may represent a hypomorphic allele with partial residual function rather than a null variant. However, when R141H occurs in trans with the truncating mutation I366fsX18 (c.1098_1100 + 7del), the compound heterozygous state (*Best1*^{R141H}/*Best1*^{I366fsX18}) results in ARB, characterized by a depressed LP:DT_{ratio} and reduced visual acuity in the 14-year-old female patient [123]. Functional studies demonstrated that when this compound variant was expressed in Human Embryonic Kidney (HEK293) cells, whole-cell chloride currents were comparable to those observed in cells transfected with wild-type Best1, indicating that loss of bestrophin-1 anion channel activity is unlikely to be the primary mechanism underlying the pathophysiology of ARB in this case [123].

Clinically, EOGs reveal a severely reduced LP:DT_{ratio} in virtually all cases, irrespective of patient age, highlighting widespread RPE dysfunction. This abnormality is typically bilateral and symmetric. The degree of EOG reduction is disproportionate when compared to full-field ERG abnormalities, underlining the primary RPE involvement characteristic of ARB. The LP:DT_{ratios} have been reported to range between severely reduced [117] to 1.89 [118] with most studies reporting values of approximately 1.00 (See Supplementary Material Table S1). The most common ERG abnormalities include reduced amplitudes and delayed peak times across both dark-adapted and light-adapted responses. Younger patients often show milder or even normal ERG findings, which correlate with better visual acuity. In contrast, older patients typically exhibit more pronounced amplitude reductions and delayed implicit times. Longitudinal follow-up in some individuals confirms progressive decline, particularly in scotopic ERG components, while cone-driven responses tend to deteriorate more slowly [118, 119]. See Fig. 2 for clinical features of ARB.

Adult onset vitelliform macular dystrophy

Adult onset Vitelliform Macular Dystrophy (AVMD), is often considered part of the spectrum of dominantly inherited bestrophinopathies and typically manifests between the ages of 30 and 50 years, with a slight female predominance [124]. Patients present with characteristic vitelliform lesions, usually smaller and less pronounced than those observed in BVMD. Although initially described as autosomal dominant, many sporadic AVMD cases likely reflect autosomal dominant inheritance with incomplete penetrance. Associated genes include *PRPH2*, *BEST1*, *IMPG1*, and *IMPG2* [125], although sporadic cases have been reported with negative genotypes for these genes [126].

Although AVMD shares a considerable phenotypic overlap with BVMD, it generally follows a milder course with later onset and slower progression [127]. Most patients maintain relatively preserved central vision, and progression through the

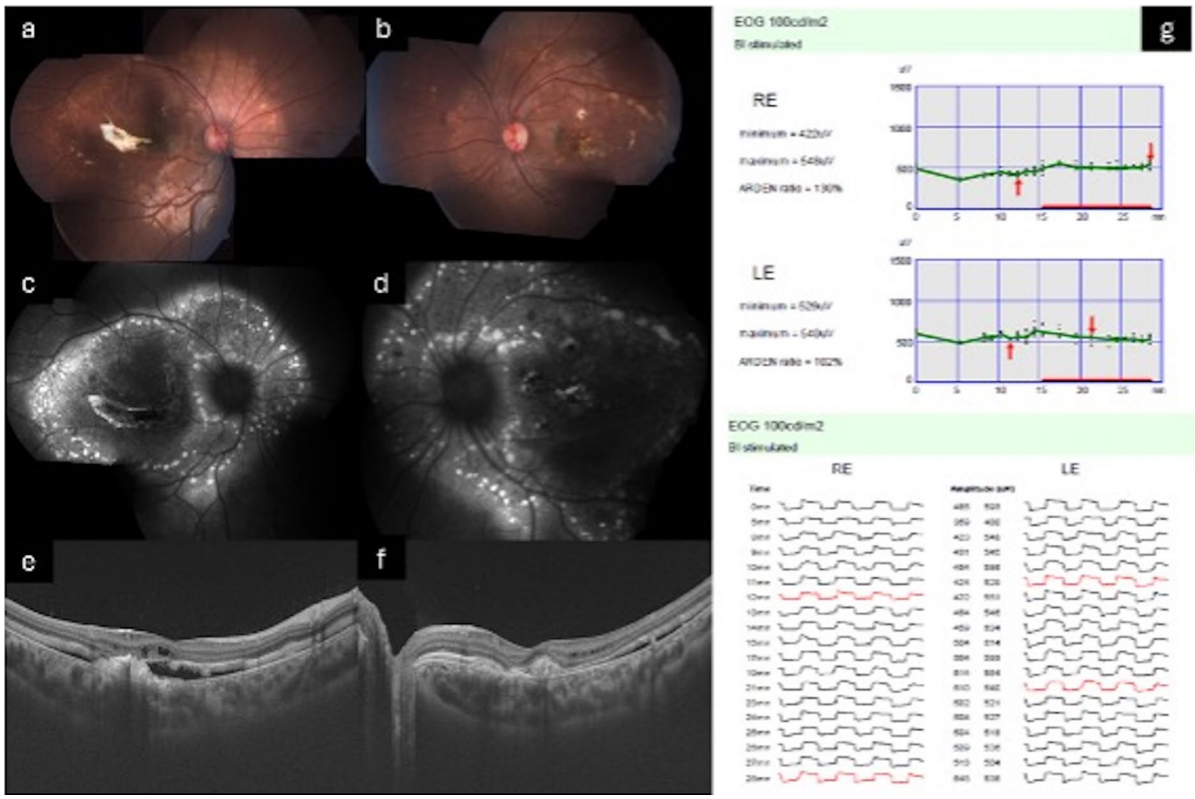

Fig. 2 **a, b** Color fundus photographs showing multiple subretinal yellow punctate lesions along the vascular arcades, peripapillary region, and nasal to the optic disc, with evidence of a scarred choroidal neovascular membrane (CNVM). **c, d** Fundus autofluorescence images demonstrating discrete areas of hyperautofluorescence corresponding to the yellow deposits seen clinically. **e, f** Swept source OCT scans revealing a subretinal hyperreflective membrane, intraretinal schisis, and a subretinal hyporeflective space. **g** Electro-oculography of both eyes showing an absent light peak, with the LP:DT 'Arden' ratios of 130% in the right eye and 102% in the left eye

classic stages of BVMD is not universal in AVMD. Nevertheless, complications such as macular atrophy and, less commonly, CNV or pigment epithelial detachment (PED) can occur [39].

Histopathological studies of AVMD are limited but have consistently demonstrated disruptions in the outer retina and RPE, with material accumulation in the subretinal space attributed to dysfunctional RPE metabolism. Reports highlight RPE hypertrophy, photoreceptor degeneration in the foveal region, pigment-laden macrophages, and the presence of periodic acid–Schiff (PAS)-positive material between the RPE and Bruch's membrane. The role of lipofuscin accumulation remains debated, with variability across studies potentially reflecting disease stage at the time of tissue sampling [17, 128–131].

Electrophysiological testing in AVMD typically reveals preserved overall retinal function with localized macular dysfunction. The ffERGs indicate normal generalized retinal responses. In contrast, mfERG consistently demonstrates reduced responses from the central macula, correlating with the focal nature of the disease [132]. Electrooculography findings are variable but usually normal or only mildly reduced, with LP:DT_{ratios} often remaining within or just below normal limits [105]. Reported values for the LP:DT_{ratio} range from normal/reduced [18] to 3.04 [22] and reported range typically lie between 1.30–1.50 (See Supplementary Material Table S1). This contrasts with BVMD, where EOG is consistently abnormal due to widespread RPE dysfunction. The electrophysiological profile of AVMD—normal ffERG and EOG with abnormal mfERG- underscores

the localized nature of the pathology and helps differentiate it from inherited bestrophinopathies such as BVMD. See Fig. 3 for clinical features of AVMD.

Future therapies

Gene therapy is emerging as a promising approach for bestrophinopathies. The human eye presents an ideal target for these therapies due to its relative immune privilege, bilateral symmetry (enabling the use of the fellow eyes as a control), and anatomical accessibility for direct visualization and monitoring [133]. The *BEST1* gene is relatively small, and its expression is restricted to the RPE, making it well-suited for delivery using adeno-associated virus (AAV) vectors. Moreover, bestrophinopathies often exhibit a slow rate of progression, providing a generous therapeutic window [104]. However, this slow and gradual progression may also impede therapeutic development by complicating endpoint detection and extending trial duration. Structural hallmarks, such as subretinal vitelliform lesions or fluid, serve as quantifiable endpoints for assessing treatment response in early-phase clinical trials using OCT, potentially enabling smaller sample sizes and streamlined regulatory pathways [62].

Preclinical evidence from animal models

Canine multifocal retinopathy (cmr), caused by naturally occurring biallelic *BEST1* pathogenic variants, closely mimics the clinical, histological, and molecular features of human ARB [134]. A study by Guziewicz et al. (2018) [135] showed that early disease in cmr is marked by micro detachments at the RPE–photoreceptor interface, linked to impaired calcium signalling and underdeveloped apical RPE microvilli. Subretinal injection of either canine or human *BEST1* using AAV vectors led to lesion reversal within 4–12 weeks and durable improvements up to 245 weeks post-injection without significant inflammation [135]. Notably, this gene replacement restored both microstructural architecture and functional adhesion at the RPE–photoreceptor junction, confirming

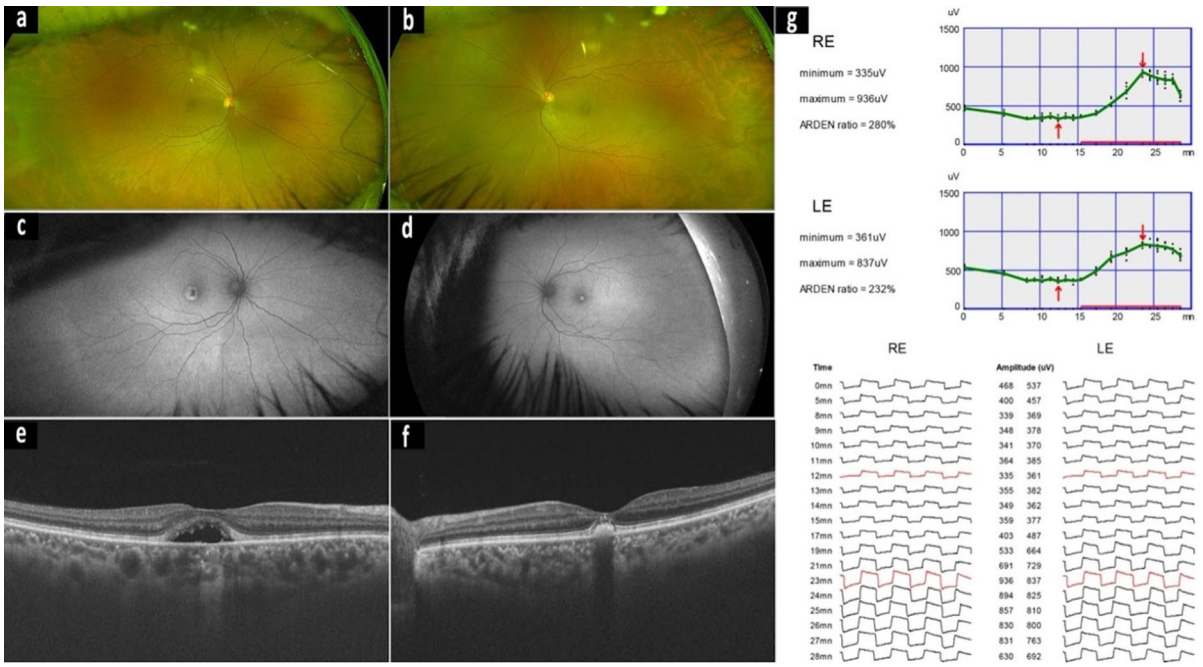

Fig. 3 A case of a 45-year-old male with adult onset foveovitelliform dystrophy. Best corrected visual acuities were 6/6 both eyes. Optus wide field colour fundus photographs **a, b** of the right and left eyes. Fundus autofluorescence (**c, d**) indicates central hyper and hypofluosecence centred on the fovea. OCT reveals a disruption to the retinal pigment epithelium and fovea with a similar pattern to BVMD. The EOGs (**g**) are within normal limits for the LP:DT 'Arden' ratio with a light-rise

the viability of this approach for early and advanced ARB.

In contrast, *BEST1*-knockout mice do not exhibit a phenotype, with a near normal normal light rise, limiting their utility [136]. However, knock-in mice harbouring the W93C disease-causing variant (seen in BVMD) demonstrate clinical features such as dominant inheritance, reduced EOG light-rise, and serous retinal detachments, making them valuable for studying dominant variants [137]. A spontaneous *BEST1* pathogenic variant *p.Q327E* has been identified in the primate *Macaca fascicularis* that could support studies into disease progression and therapeutic targets [138].

Insights from iPSC-RPE models

Patient-derived induced pluripotent stem cells (iPSCs), differentiated into RPE, offer a powerful in vitro platform for modelling disease and testing therapy. These iPSC-RPEs recapitulate disease-specific defects in *BEST1*-mediated chloride conductance and permit pathogenic variant-specific assessments. Baculovirus-mediated supplementation has rescued Cl^- currents in ARB iPSC-RPEs [74]. Furthermore, dominant disease-causing variants-if not GOF-can be effectively rescued by overexpressing wild-type (WT) *BEST1*, supported by the tolerability of *BEST1* overexpression in canine models [59]. Notably, both recessive and dominant pathogenic variants with LOF or dominant-negative (DN) behaviour-but without toxic GOF effects-are amenable to gene augmentation therapy using AAV, lentiviral, or baculoviral vectors [59]. Restoration of chloride channel function is often dose- and time-dependent, regardless of inheritance pattern [76].

Overcoming gain-of-function challenges

Some dominant *BEST1* disease-causing variants exert a DN effect via toxic GOF, which resists simple gene supplementation. These cases require a *silence-and-replace* approach. CRISPR/Cas9-based vectors have been employed to suppress endogenous mutant *BEST1* expression (non-selective or allele-specific), coupled with exogenous WT gene delivery [76, 139]. This dual strategy successfully restored normal chloride channel function in iPSC-RPEs carrying three different GOF pathogenic variants, establishing feasibility for broad application across bestrophinopathy variants [74, 76, 135].

Functional assay for AAV-*BEST1* in cell lines

A key advancement supporting clinical translation of *BEST1* gene therapy is the development of a functional in vitro assay using HEK293 cells. This assay measures chloride conductance via whole-cell patch-clamp to confirm the efficacy of AAV-mediated *BEST1* delivery. Protein expression correlates with functional activity, and the inclusion of the WPRE (Woodchuck Hepatitis Virus Post-transcriptional Regulatory Element) enhances both. This reproducible and GMP-compatible assay serves as a critical potency and quality control tool for future clinical trials [58].

Pharmacological therapy for bestrophinopathies

While genomic therapies have dominated recent research, pharmacological approaches remain valid and promising. Valproic acid, in combination with rapamycin, has been shown to modulate proteolytic machinery and rescue photoreceptor outer segment processing defects in patient-derived iPSC-RPE, while also reducing autofluorescent material and delaying disease progression in canine models of ARB [140]. Additionally, molecular chaperones and proteasome inhibitors such as bortezomib and 4-phenylbutyrate (4PBA) have demonstrated the ability to correct trafficking of mutant *BEST1* and restore channel activity in cell models. 4PBA and its analogue 2-naphthoxyacetic acid have further shown efficacy in enhancing *BEST1* expression and chloride conductance in both patient-derived iPSC-RPE and HEK293 cells [66]. Despite their potential, many pharmacological agents require high concentrations and exhibit pathogenic variant-specific variability, highlighting the need for more tailored strategies. Table 1 summarises clinical trials targeting the bestrophinopathies. See also Supplementary Material Table S2 for ADVIRC clinical trials.

Table 1 Summary of clinical trials targeting *BEST1* pathogenic variants. *Source* www.clinicaltrials.gov

Gene / Drug Strategy	Vector/ Delivery	Clinical Condition	Inheritance / Mechanism	Disease Model / Population	Outcome
Gene augmentation [62]	Baculovirus vector	ARB	Autosomal recessive	iPSC-RPE cells	Rescue of Ca^{2+}-dependent Cl^- current (whole-cell patch clamp)
Gene augmentation [113]	AAV2 vector	ARB (canine model)	Autosomal recessive	Canine BEST1 disease model	Reversal of subretinal detachment and micro detachment; correction of PR/RPE interface
Gene augmentation [116]	Lentiviral vector	ARB	Autosomal recessive	iPSC-RPE cells	Increased BEST1 protein; restoration of Ca^{2+}-activated Cl^- current; improved RPE function (rhodopsin degradation)
Gene augmentation [116]	Lentiviral vector	BVMD	Autosomal dominant	iPSC-RPE cells	Increased BEST1 protein; restoration of Ca^{2+}-activated Cl^- current; improved RPE function
CRISPR/Cas9-mediated knock-out of mutant allele [116]	Lentiviral vector (Cas9 + sgRNA)	BVMD	Autosomal dominant	iPSC-RPE cells	Increased BEST1 protein; restoration of Ca^{2+}-activated Cl^- current
Gene augmentation [50]	AAV2 vector / Baculovirus vector	BVMD	Autosomal dominant (loss-of-function)	iPSC-RPE	Rescue of Ca^{2+}-dependent Cl^- current (whole-cell patch clamp)
CRISPR/dCas9-mediated knock-down of both alleles + gene augmentation [67]	(i) Baculovirus expressing dCas9-KRAB-MeCP2; (ii) Baculovirus expressing WT BEST1	*BEST1*-related diseases	Autosomal dominant (gain-of-function)	hPSC-RPE H1-iCas9 cells	Rescue of Ca^{2+}-dependent Cl^- current
Gene augmentation (OPGx-BEST1) NCT07185256	AAV-based vector; single subretinal injection	BVMD and ARB (BIRD-1 Phase 1/2 trial, NCT07185256)	BEST1-related IRD (AD BVMD and AR ARB)	Adult patients (≥ 18 years) with BVMD or ARB due to BEST1 mutations	Ongoing multi-center, adaptive, open-label, dose-exploring Phase 1b/2a trial; primary endpoints: safety and tolerability over 5 years; secondary/exploratory endpoints: dose finding and preliminary efficacy (visual function, retinal structure)

Table 1 (continued)

Gene / Drug Strategy	Vector/ Delivery	Clinical Condition	Inheritance / Mechanism	Disease Model / Population	Outcome
Natural history / registry (non-interventional, trial-enabling) NCT05809635	Standard clinical imaging and functional testing	BVMD	*BEST1* mutations (various AD/AR)	Children and adults with BEST1 VMD	Prospective natural history and genotype–phenotype correlation to support endpoint selection and trial design; no therapeutic intervention

The clinical electrooculogram

The clinical EOG was described by Arden et al. (1962) [141]who proposed that the LP:DT_{ratio} could be used as a test of retinal function based on previous studies that investigated the interactions of light and the standing potential in retinal disease [141–143]. The standard model for the light-rise is based on an interaction between the rods and RPE and includes a 'light-rise' substance that is released from the dark adapted rods which either binds to or permeates the RPE to increase the basolateral membrane conductance which results in a positive shift in the recorded standing potential of the eye [50, 52, 75, 141]. The clinical EOG has been standardized since 1993 [144] when the protocol of dark adaptation followed by light adaptation to record the changes in the standing potential of the eye during saccadic eye movements at minute intervals was established.

The standing potential is the corneo-fundal potential [145] that has a positive value by convention and is generated principally across the RPE [146]. The clinical features of the EOG include the fall in the standing potential during a period of dark adaptation forming a 'dark trough' (DT). The DT minimum occurs ~ 10–15 min during the 15-min dark adaptation period. Following a 15-min period of white light adaptation of 100 cd/m^2 background luminance the standing potential increases (termed the 'light-rise') to reach a maximum 'light peak' (LP) at approximately 7–12 min before declining again [1]. Clinically the main measure used is the ratio of the LP:DT formally known as the Arden Index or Arden ratio and from a meta-analysis has a mean value of 2.35 (95% CI 2.28–2.42) in dilated subjects and a mean value of 2.37 (95% CI 2.28–2.45) in nondilated subjects [147].

Adapted clinical electrooculogram protocols

According to the ISCEV standard the clinical EOG involves recording of the standing potential of the eye through eye movements and alternating fixation during a 15-min dark-adaptation period, followed by an additional 15 min of measurement in light-adapted conditions [1, 52, 141]. EOG recording procedure is simple, but it is prone to artefacts, especially due to irregular eye movements or changes of

posture during the examination. Such difficulties are frequently attributed to the prolonged and monotonous nature of the examination, which can lead to diminished concentration, discomfort, and fatigue of the patients. Furthermore, in pediatric and disabled patient populations, maintaining stable eye movements throughout the full 30-min recording session may not always be feasible. Thus, shorter-duration tests may be beneficial as they may be better tolerated in certain clinical circumstances while reducing the testing burden on the patient.

Türksever et al. (2015) [49] were the first to demonstrate the feasibility of short-duration EOG recording. Their recording protocol comprised a total dark phase duration of 10 min, consisting of 6 min of pre-adaptation to the dark, followed by 4 min of alternating fixation. A light phase was established with a total duration of 14 min, which included 4 min of light adaptation followed by 10 min of alternating fixation. Their work considered previously identified physiological factors that influenced the amplitude of the DT and LP [141–143]. As such, the recorded characteristics of this short-duration EOG protocol closely resembled those of the ISCEV standard EOG recordings. The median values of LP:DT_{ratio} were 2.25 and 2.4 (according to age-group), with the respective lower confidence limit between 1.60 and 1.77, which is equal to the values specified in the current ISCEV Standard (typically ranging from 1.7 to 4.3) [1].

The clinical EOG is usually conducted as only one of a broader set of tests within routine electrophysiological assessments. Simultaneous recording of ffERG is often necessary, to ensure accurate interpretation of EOG findings by excluding potential rod dysfunction. The need to perform both tests not only prolongs the overall duration of the electrophysiological assessment but also exacerbates patient discomfort. Djukanović et al. (2024) [48] attempted to further shorten the duration of testing by combining both examinations into one. Their protocol was based on the understanding that both EOG and ffERG require periods of dark and light adaptation. The primary output of the EOG test, specifically the LP:DT_{ratio}, corresponds to critical time points during the dark and light adaptation phases when DT and LP are expected. If these two time points are evaluated during the dark and light adaptation periods within ffERG testing, then simultaneous EOG testing is possible (see Fig. 4). The EOG protocol was called a screening EOG because it consisted of only two recordings of the standing potential in the dark, and two in the light, but demonstrated clinical results that were comparable to the standard ISCEV EOG, with similar sensitivity and specificity in identifying RPE dysfunction in patients diagnosed with BVMD [48].

However, the screening EOG protocol according to Djukanovic et al. (2024) [48] gave slightly lower values in the control population compared to the standard EOG (1.98 ± 0.33 with screening EOG vs. 2.67 ± 0.61 with standard protocol) and lower than those reported by Türksever et al. (2015) [49]. This discrepancy may have arisen due to several factors, the first was that the simultaneous measurement of ffERG responses, performed by Djukanovic et al. (2024) [48]may have influenced the result of the screening EOG. During the dark phase of their protocol, the retina was partially stimulated by relatively intense flashes of dark-adapted ERG recordings. Besides, background luminance for the light phase of the screening EOG was aligned with the ffERG, which, however, requires lower luminance than those recommended for standard EOG (30 cd/m^2 for ffERG vs. 100 cd/m^2 for EOG). Furthermore, Djukanovic et al. (2024) [48] measured the standing potential in one-time point only, which may have contributed to less precise assessment of significant changes, as individual variations in the appearance of the LP and DT time points are likely to occur. Further improvements of integrated methodology could be obtained if the protocol implemented by Türksever et al. (2015) [49] (dark phase: 6 min of adaptation, 4 min of alternating fixation; light phase: 4 min of light adaptation, 10 min of alternating fixation) would be integrated into the ffERG investigation. Such a protocol could maintain the precision of standard methodology while reducing the testing burden on the patient, as attempted by Djukanovic et al. (2024) [48].

Fast oscillation

One additional test, that is not commonly performed, is the Fast Oscillation (FO) of the ocular standing potential. In the FO the standing potential reduces during the light phase and increases in amplitude during the dark phase that originates in the RPE [148]. In contrast to the clinical EOG the dark and light phase intervals are 1 min in duration and typically

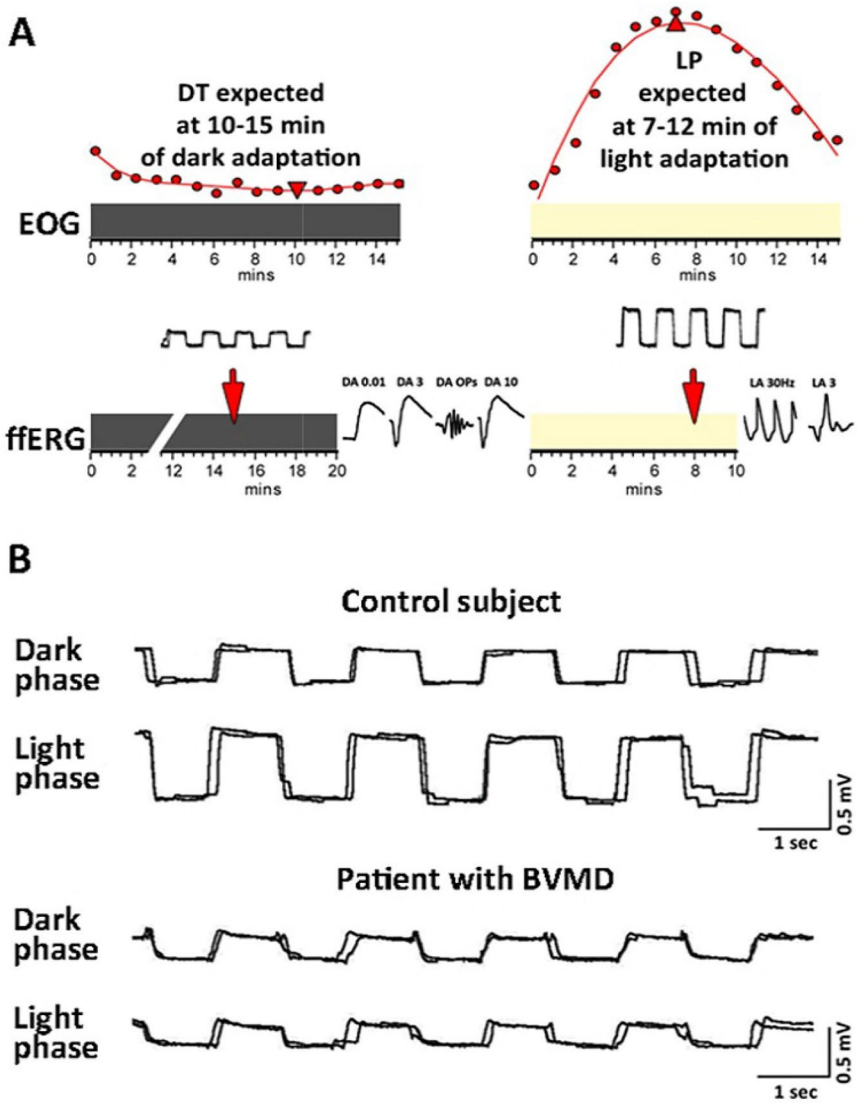

Fig. 4 **A** The concept of integrating screening electrooculography (EOG) into the ffERG examination, as presented in the study by Djukanovic et al. (2024) [48]. The dark line represents dark adaptation, and the light line represents light adaptation. DT -dark trough, LP—light peak. **B** The recordings obtained from screening EOG during dark and light adaptation. In the control subject, a notable increase in the standing potential was observed during the light phase, while in a patient diagnosed with Best Vitelliform Macular Dystrophy (BVMD), the standing potential did not increase during light adaptation

4–5 cycles are recorded taking approximately 10 min to complete the test. The fall in the standing potential during the light phase is due to the delayed basolateral membrane hyperpolarization [149–151] caused by a fall in sub retinal potassium following light absorption by the photoreceptors and inhibition of the outward potassium current mainly from the inner segments [152, 153]. The reduction in sub-retinal potassium slows the apical NaK2Cl cotransporter reducing the intracellular chloride concentration and basolateral chloride conductance resulting in the hyperpolarization of the basolateral membrane which causes a fall in the standing potential that reaches a minimum approximately 30 s after light onset [154]. The FO is not routinely recorded clinically but has been shown to have a larger amplitude following acute increase in blood glucose levels [155] and reduced in diabetes [156]. The FO is unaffected in BVMD [157] but may serve as a functional test for homeostasis of fluid in the sub-retinal; space given its dependence on NaK2Cl co-transporter. For recording the FO see the ISCEV EOG standard [1] and Mergaerts et al. (2001) [158]. The FO is also demanding on the patient with continuous saccades required to be performed during the light and dark cycles over 10–12 min. Modifications to the recommended protocol to reduce the number of cycles and/or the timing of the saccadic recording intervals to the anticipated peaks and

troughs may lead to the FO being utilized more frequently clinically in the future.

Discussion

The bestrophinopathies represent a clinically and genetically heterogeneous group of inherited retinal disorders that can be assessed using the EOG [6, 8]. This companion review to the mechanism of the EOG, provides an overview of disease-causing variants in *BEST1* can give rise to a spectrum of phenotypes ranging from the classic vitelliform lesions of BVMD to peripheral retinal changes seen in ADVRIC, and the multifocal presentations characteristic of ARB [7, 9, 42]. One unifying finding across these conditions is the abnormal EOG light-rise, reflecting widespread RPE dysfunction that may not correlate with the clinical appearance [39, 116]. Whilst genotype–phenotype correlations remain complex [43–45], the common EOG abnormalities provide a functional clinical marker that points to the role of bestrophin-1 in maintaining RPE physiology through regulation of intracellular calcium [11, 12].

Some potential therapeutic approaches for the bestrophinopathies, include gene therapies in canine models using AAV vectors that have restored *BEST1* function with structural and functional changes lasting several years [63, 135]. In addition, patient-derived iPSC-RPE models have enabled the identification and testing of potential therapeutic interventions by providing disease-causing variant-specific platforms for testing both gene replacement and pharmacological interventions [66, 69, 71–73, 76]. The distinction between LOF and GOF pathogenic variants has informed the development of tailored therapeutic strategies, with simple gene augmentation proving effective for most variants, while DN variants require more sophisticated "silence-and-replace" approaches using CRISPR-Cas9 technology [76, 139]. In addition, small molecule therapeutics, including 4-phenylbutyrate and tadalafil, offers clinical interventions to further support restoration of *BEST1* function [64, 66].

The clinical utility of the EOG in diagnosing bestrophinopathies is established but extending the current clinical utility of the EOG could be enhanced if the testing time was reduced from the current recommended 30 min [1]. The suggestion of using alternative shortened EOG protocols, even if as a screening instrument, represent a step towards making the EOG a more accessible and patient-friendly [48, 49]. The successful implementation of 10–14-min protocols that reduce test time [49] as well as integrating EOG recording within the ISCEV standard ERG protocol [48], may support wider use of the EOG as part of routine electrophysiological assessment during standard electrophysiological assessment.

The use of the EOG may increase to monitor outcomes for novel gene or therapeutic therapies that target the bestrophinopathies [62] in conjunction with structural imaging of the RPE [104]. From the first description of the clinical EOG by Arden et al. (1962) [141] that was standardized in the first ISCEV EOG standard [144] there have been no major amendments to the clinical recording. Now, strategies to reduce testing time of the EOG [48, 49] may provide an impetus to develop a shortened EOG test protocol. Modifications to the wavelength using a short wavelength 30 cd/m^2 [159] stimulus may also offer a new testing strategy to be devised and validated [160]. If as the companion paper suggests that the light-rise reflects the availability of ATP and the metabolic health of the RPE then the EOG may find additional uses in evaluating the functional integrity of the EOG in a short and patient friendly protocol.

The last major review of the electrooculogram was by Arden and Constable (2006) [52] which predated the understanding of bestrophin's role as a intracellular Ca^{2+} regulator and the identification of anoctamin ion channels in the RPE that is discussed in the companion paper. With the EOG and FO being the only functional electrophysiological tests with which to identify central RPE pathology and the development of therapeutics targeting the RPE, these clinical test protocols could be revised to improve patient comfort, clinical utility and improved service delivery [161]. The intention of this and the companion paper is to provide an update on the EOG mechanism and suggest a central role for ATP in the generation of the light-rise. In addition, emphasising the need to further test and refine the proposed shortened [49], screening [48] and short wavelength at 30 cd/m^2 [159, 160] stimuli in clinical populations to develop a modified EOG protocol.

Acknowledgements None

Author contributions All authors contributed to the first draft and all authors read and approved the final manuscript.

Funding Open Access funding enabled and organized by CAUL and its Member Institutions. None.

Data availability No datasets were generated or analysed during the current study.

Code availability Not Applicable.

Declarations

Conflict of interest The authors declare no competing interests.

Ethical approval Not applicable.

Consent to Participate Not applicable.

Consent for Publication All participants gave consent to publish anonymised data obtained from their clinical records.

Statement of human rights All procedures performed in study involving human participants were in accordance with the ethical standards of institutional and/or national research committee and with the 1964 Helsinki declaration and its later amendments or comparable ethical standards.

Statement on the welfare of animals Not applicable.

Informed consent Not applicable.

References

1. Constable PA, Bach M, Frishman LJ, Jeffrey BG, Robson AG (2017) International society for clinical electrophysiology of vision ISCEV standard for clinical electro-oculography (2017 update). Doc Ophthalmol 134:1–9. https://doi.org/10.1007/s10633-017-9573-2
2. Strauss O (2005) The retinal pigment epithelium in visual function. Physiol Rev 85:845–881. https://doi.org/10.1152/physrev.00021.2004
3. Panda-Jonas S, Jonas JB, Jakobczyk-Zmija M (1996) Retinal pigment epithelial cell count, distribution, and correlations in normal human eyes. Am J Ophthalmol 121:181–189. https://doi.org/10.1016/s0002-9394(14)70583-5
4. Fields MA, Del Priore LV, Adelman RA, Rizzolo LJ (2020) Interactions of the choroid, Bruch's membrane, retinal pigment epithelium, and neurosensory retina collaborate to form the outer blood-retinal-barrier. Prog Retin Eye Res 76:100803. https://doi.org/10.1016/j.preteyeres.2019.100803
5. Rizzolo LJ (2007) Development and role of tight junctions in the retinal pigment epithelium. Int Rev Cytol 258:195–234. https://doi.org/10.1016/S0074-7696(07)58004-6
6. Guziewicz KE, Sinha D, Gómez NM et al (2017) Bestrophinopathy: an RPE-photoreceptor interface disease. Prog Retin Eye Res 58:70–88. https://doi.org/10.1016/j.preteyeres.2017.01.005
7. Leroy BP (2012) Bestrophinopathies. In: El T (ed) Genetic diseases of the eye. Oxford University Press, Oxford, pp 426–436
8. Johnson AA, Guziewicz KE, Lee CJ et al (2017) Bestrophin 1 and retinal disease. Prog Retin Eye Res 58:45–69. https://doi.org/10.1016/j.preteyeres.2017.01.006
9. Shah M, Broadgate S, Shanks M et al (2020) Association of clinical and genetic heterogeneity with *BEST1* sequence variations. JAMA Ophthalmol 138:544–551. https://doi.org/10.1001/jamaophthalmol.2020.0666
10. Strauß O, Reichhart N, Gomez NM, Müller C (2016) Contribution of ion channels in calcium signaling regulating phagocytosis: MaxiK, Cav1.3 and Bestrophin-1. Adv Exp Med Biol 854:739–744. https://doi.org/10.1007/978-3-319-17121-0_98
11. Müller C, Más Gómez N, Ruth P, Strauss O (2014) $Ca_V1.3$ L-type channels, maxiK Ca^{2+}-dependent K^+ channels and bestrophin-1 regulate rhythmic photoreceptor outer segment phagocytosis by retinal pigment epithelial cells. Cell Signal 26:968–978. https://doi.org/10.1016/j.cellsig.2013.12.021
12. Milenkovic A, Brandl C, Milenkovic VM et al (2015) Bestrophin 1 is indispensable for volume regulation in human retinal pigment epithelium cells. Proc Natl Acad Sci USA 112:E2630–E2639. https://doi.org/10.1073/pnas.1418840112
13. Cordes M, Bucichowski P, Alfaar AS et al (2020) Inhibition of Ca^{2+} channel surface expression by mutant bestrophin-1 in RPE cells. FASEB J 34:4055–4071. https://doi.org/10.1096/fj.201901202RR
14. Davidson AE, Millar ID, Urquhart JE et al (2009) Missense mutations in a retinal pigment epithelium protein, bestrophin-1, cause retinitis pigmentosa. Am J Hum Genet 85:581–592. https://doi.org/10.1016/j.ajhg.2009.09.015
15. Mullins RF, Kuehn MH, Faidley EA, Syed NA, Stone EM (2007) Differential macular and peripheral expression of bestrophin in human eyes and its implication for

Best disease. Invest Ophthalmol Vis Sci 48:3372–3380. https://doi.org/10.1167/iovs.06-0868
16. Greaves AH, Sarks JP, Sarks SH (1990) Adult vitelliform macular degeneration: a clinical spectrum. Aust N Z J Ophthalmol 18:171–178. https://doi.org/10.1111/j.1442-9071.1990.tb00610.x
17. Gass JD (1974) A clinicopathologic study of a peculiar foveomacular dystrophy. Trans Am Ophthalmol Soc 72:139–156
18. Meunier I, Sénéchal A, Dhaenens CM et al (2011) Systematic screening of *BEST1* and *PRPH2* in juvenile and adult vitelliform macular dystrophies: a rationale for molecular analysis. Ophthalmology 118:1130–1136. https://doi.org/10.1016/j.ophtha.2010.10.010
19. Chowers I, Tiosano L, Audo I, Grunin M, Boon CJ (2015) Adult-onset foveomacular vitelliform dystrophy: a fresh perspective. Prog Retin Eye Res 47:64–85. https://doi.org/10.1016/j.preteyeres.2015.02.001
20. Meunier I, Manes G, Bocquet B et al (2014) Frequency and clinical pattern of vitelliform macular dystrophy caused by mutations of interphotoreceptor matrix *IMPG1* and *IMPG2* genes. Ophthalmology 121:2406–2414. https://doi.org/10.1016/j.ophtha.2014.06.028
21. Manes G, Meunier I, Avila-Fernández A et al (2013) Mutations in *IMPG1* cause vitelliform macular dystrophies. Am J Hum Genet 93:571–578. https://doi.org/10.1016/j.ajhg.2013.07.018
22. Vázquez-Domínguez I, Li CHZ, Fadaie Z et al (2022) Identification of a complex allele in *IMPG2* as a cause of adult-onset vitelliform macular dystrophy. Invest Ophthalmol Vis Sci 63:27. https://doi.org/10.1167/iovs.63.5.27
23. Jaouni T, Averbukh E, Burstyn-Cohen T et al (2012) Association of pattern dystrophy with an *HTRA1* single-nucleotide polymorphism. Arch Ophthalmol 130:987–991. https://doi.org/10.1001/archophthalmol.2012.1483
24. Alexis JA, Ramakrishnan P, Kenworthy MK, Thompson JA, Chelva ES, Chen FK (2025) *CTNNA1*-associated retinal dystrophy: novel multimodal imaging and electrophysiology features. Doc Ophthalmol 151:239–246. https://doi.org/10.1007/s10633-025-10027-0
25. Miller SA, Stevens TS, Myers F, Nieder M (1978) Pigmented paravenous retinochoroidal atrophy. Ann Ophthalmol 10:867–871
26. Smith VC, Pokorny J, Ernest JT, Starr SJ (1978) Visual function in acute posterior multifocal placoid pigment epitheliopathy. Am J Ophthalmol 85:192–199. https://doi.org/10.1016/s0002-9394(14)75947-1
27. Marmor MF, McNamara JA (1996) Pattern dystrophy of the retinal pigment epithelium and geographic atrophy of the macula. Am J Ophthalmol 122:382–392. https://doi.org/10.1016/s0002-9394(14)72065-3
28. Stavrou P, Good PA, Broadhurst EJ, Bundey S, Fielder AR, Crews SJ (1996) ERG and EOG abnormalities in carriers of X-linked retinitis pigmentosa. Eye 10(Pt 5):581–589. https://doi.org/10.1038/eye.1996.134
29. Kim RY, Faktorovich EG, Kuo CY, Olson JL (1997) Retinal function abnormalities in membranoproliferative glomerulonephritis type II. Am J Ophthalmol 123:619–628. https://doi.org/10.1016/s0002-9394(14)71074-8
30. Kellner U, Weleber RG, Kennaway NG, Fishman GA, Foerster MH (1997) Gyrate atrophy-like phenotype with normal plasma ornithine. Retina 17:403–413. https://doi.org/10.1097/00006982-199709000-00008
31. Eysteinsson T, Jónasson F, Jónsson V, Bird AC (1998) Helicoidal peripapillary chorioretinal degeneration: electrophysiology and psychophysics in 17 patients. Br J Ophthalmol 82:280–285. https://doi.org/10.1136/bjo.82.3.280
32. Lam BL, Lopez PF, Dubovy SR, Liu M (2009) Transient electro-oculogram impairment in unilateral acute idiopathic maculopathy. Doc Ophthalmol 119:157–161. https://doi.org/10.1007/s10633-009-9179-4
33. Small KW, Jampol LM, Bakall B et al (2022) Best vitelliform macular dystrophy (BVMD) is a phenocopy of north carolina macular dystrophy (NCMD/MCDR1). Ophthalmic Genet 43:307–317. https://doi.org/10.1080/13816810.2021.2010771
34. Thompson DA, Constable PA, Liasis A, Walters B, Esteban MT (2016) The physiology of the retinal pigment epithelium in Danon disease. Retina 36:629–638. https://doi.org/10.1097/IAE.0000000000000736
35. Dahanayake P, Dassanayake TL, Pathirage M, Senanayake S, Sedgwick M, Weerasinghe V (2020) Electro-oculography in bilateral optic neuropathy. BMC Res Notes 13:287. https://doi.org/10.1186/s13104-020-05131-0
36. Arndt CF, Derambure P, Defoort-Dhellemmes S, Hache JC (1999) Outer retinal dysfunction in patients treated with vigabatrin. Neurology 52:1201–1205. https://doi.org/10.1212/wnl.52.6.1201
37. Neubauer AS, Samari-Kermani K, Schaller U, Welge-Lübetaen U, Rudolph G, Berninger T (2003) Detecting chloroquine retinopathy: electro-oculogram versus colour vision. Br J Ophthalmol 87:902–908. https://doi.org/10.1136/bjo.87.7.902
38. Wang L, Miao H, Li X (2015) Tamoxifen retinopathy: a case report. Springerplus 4:501. https://doi.org/10.1186/s40064-015-1258-2
39. Boon CJ, Klevering BJ, Leroy BP, Hoyng CB, Keunen JE, den Hollander AI (2009) The spectrum of ocular phenotypes caused by mutations in the *BEST1* gene. Prog Retin Eye Res 28:187–205. https://doi.org/10.1016/j.preteyeres.2009.04.002
40. Qian CX, Charran D, Strong CR, Steffens TJ, Jayasundera T, Heckenlively JR (2017) Optical coherence tomography examination of the retinal pigment epithelium in best vitelliform macular dystrophy. Ophthalmology 124:456–463. https://doi.org/10.1016/j.ophtha.2016.11.022
41. Augstburger E, Orès R, Mohand-Said S et al (2019) Outer retinal alterations associated with visual outcomes in best vitelliform macular dystrophy. Am J Ophthalmol 208:429–437. https://doi.org/10.1016/j.ajo.2019.08.011
42. Nachtigal AL, Milenkovic A, Brandl C et al (2020) Mutation-dependent pathomechanisms determine the phenotype in the bestrophinopathies. Int J Mol Sci 21:1597. https://doi.org/10.3390/ijms21051597
43. Wang Y, Jiang Y, Li X et al (2022) Genetic and clinical features of *BEST1*-associated retinopathy based on 59

Chinese families and database comparisons. Exp Eye Res 223:109217. https://doi.org/10.1016/j.exer.2022.109217
44. Frecer V, Iarossi G, Salvetti AP et al (2019) Pathogenicity of new *BEST1* variants identified in Italian patients with Best vitelliform macular dystrophy assessed by computational structural biology. J Transl Med 17:330. https://doi.org/10.1186/s12967-019-2080-3
45. Laich Y, Georgiou M, Fujinami K et al (2024) Best Vitelliform Macular Dystrophy natural history study report 1: clinical features and genetic findings. Ophthalmology 131:845–854. https://doi.org/10.1016/j.ophtha.2024.01.027
46. Laich Y, Georgiou M, Fujinami K et al (2025) Best vitelliform macular dystrophy natural history study report 2: fundus autofluorescence and OCT. Ophthalmol Retina 9:899–907. https://doi.org/10.1016/j.oret.2025.03.004
47. Bitner H, Schatz P, Mizrahi-Meissonnier L, Sharon D, Rosenberg T (2012) Frequency, genotype, and clinical spectrum of Best vitelliform macular dystrophy: data from a national center in Denmark. Am J Ophthalmol 154:403-412.e4. https://doi.org/10.1016/j.ajo.2012.02.036
48. Djukanovic P, Jarc Vidmar M, Sustar Habjan M (2024) Screening electro-oculography protocol as a part of full-field electroretinography. Doc Ophthalmol 149:143–150. https://doi.org/10.1007/s10633-024-09994-7
49. Türksever C, Orgül S, Todorova MG (2015) Comparing short-duration electro-oculograms with and without mydriasis in healthy subjects. Klin Monbl Augenheilkd 232:471–476. https://doi.org/10.1055/s-0034-1396330
50. Constable PA (2024) The clinical electro-oculogram. In: Das T, Satgunam P (eds) Ophthalmic diagnostics. Springer, Singapore, pp 449–461
51. Constable PA (2014) A perspective on the mechanism of the light-rise of the electrooculogram. Invest Ophthalmol Vis Sci 55:2669–2673. https://doi.org/10.1167/iovs.14-13979
52. Arden GB, Constable PA (2006) The electro-oculogram. Prog Retin Eye Res 25:207–248. https://doi.org/10.1016/j.preteyeres.2005.11.001
53. Schatz P, Klar J, Andréasson S, Ponjavic V, Dahl N (2006) Variant phenotype of Best vitelliform macular dystrophy associated with compound heterozygous mutations in *VMD2*. Ophthalmic Genet 27:51–56. https://doi.org/10.1080/13816810600677990
54. Sohn EH, Francis PJ, Duncan JL et al (2009) Phenotypic variability due to a novel Glu292Lys variation in exon 8 of the *BEST1* gene causing Best macular dystrophy. Arch Ophthalmol 127:913–920. https://doi.org/10.1001/archophthalmol.2009.148
55. Johnson AA, Lee YS, Stanton JB et al (2013) Differential effects of Best disease causing missense mutations on bestrophin-1 trafficking. Hum Mol Genet 22:4688–4697. https://doi.org/10.1093/hmg/ddt316
56. Doumanov JA, Zeitz C, Dominguez Gimenez P et al (2013) Disease-causing mutations in *BEST1* gene are associated with altered sorting of bestrophin-1 protein. Int J Mol Sci 14:15121–15140. https://doi.org/10.3390/ijms140715121
57. Milenkovic VM, Röhrl E, Weber BH, Strauss O (2011) Disease-associated missense mutations in bestrophin-1 affect cellular trafficking and anion conductance. J Cell Sci 124(Pt 17):2988–2996. https://doi.org/10.1242/jcs.085878
58. Amato A, Wongchaisuwat N, Lamborn A et al (2023) Gene therapy in bestrophinopathies: insights from preclinical studies in preparation for clinical trials. Saudi J Ophthalmol 37:287–295. https://doi.org/10.4103/sjopt.sjopt_175_23
59. Ji C, Li Y, Kittredge A et al (2019) Investigation and restoration of BEST1 activity in patient-derived RPEs with dominant mutations. Sci Rep 9:19026. https://doi.org/10.1038/s41598-019-54892-7
60. Wood SR, McClements ME, de la Martinez-Fernandez Camara C et al (2019) A quantitative chloride channel conductance assay for efficacy testing of AAV.BEST1. Hum Gene Ther Methods 30:44–52. https://doi.org/10.1089/hgtb.2018.267
61. Kittredge A, Ward N, Hopiavuori A, Zhang Y, Yang T (2018) Expression and purification of mammalian bestrophin ion channels. J Vis Exp. https://doi.org/10.3791/57832
62. Yang T, Justus S, Li Y, Tsang SH (2015) BEST1: the best target for gene and cell therapies. Mol Ther 23:1805–1809. https://doi.org/10.1038/mt.2015.177
63. Guziewicz KE, Zangerl B, Komáromy AM et al (2013) Recombinant AAV-mediated *BEST1* transfer to the retinal pigment epithelium: analysis of serotype-dependent retinal effects. PLoS ONE 8:e75666. https://doi.org/10.1371/journal.pone.0075666
64. Elverson K, Warwicker J, Freeman S, Manson F (2023) Tadalafil rescues the p.M325T mutant of Best1 chloride channel. Molecules 28:3317. https://doi.org/10.3390/molecules28083317
65. Uggenti C, Briant K, Streit AK et al (2016) Restoration of mutant bestrophin-1 expression, localisation and function in a polarised epithelial cell model. Dis Model Mech 9:1317–1328. https://doi.org/10.1242/dmm.024216
66. Liu J, Taylor RL, Baines RA et al (2020) Small molecules restore bestrophin 1 expression and function of both dominant and recessive bestrophinopathies in patient-derived retinal pigment epithelium. Invest Ophthalmol Vis Sci 61:28. https://doi.org/10.1167/iovs.61.5.28
67. Lin TC, Lin YY, Hsu CC et al (2019) Nanomedicine-based curcumin approach improved ROS damage in Best dystrophy-specific induced pluripotent stem cells. Cell Transplant 28:1345–1357. https://doi.org/10.1177/0963689719860130
68. Lee TK, Clandinin MT, Hébert M, MacDonald IM (2010) Effect of docosahexaenoic acid supplementation on the macular function of patients with best vitelliform macular dystrophy: randomized clinical trial. Can J Ophthalmol 45:514–519. https://doi.org/10.3129/i10-028
69. Kittredge A, Zhang Y, Yang T (2021) Evaluating BEST1 mutations in pluripotent stem cell-derived retinal pigment epithelial cells. Methods Enzymol 654:365–382. https://doi.org/10.1016/bs.mie.2021.01.004
70. Gao T, Tian C, Xu H, Tang X, Huang L, Zhao M (2020) Disease-causing mutations associated with

bestrophinopathies promote apoptosis in retinal pigment epithelium cells. Graefes Arch Clin Exp Ophthalmol 258:2251–2261. https://doi.org/10.1007/s00417-020-04636-5
71. Singh R, Shen W, Kuai D et al (2013) iPS cell modeling of Best disease: insights into the pathophysiology of an inherited macular degeneration. Hum Mol Genet 22:593–607. https://doi.org/10.1093/hmg/dds469
72. Kittredge A, Ji C, Zhang Y, Yang T (2018) Differentiation, maintenance, and analysis of human retinal pigment epithelium cells: a disease-in-a-dish model for *BEST1* mutations. J Vis Exp 2018:57791. https://doi.org/10.3791/57791
73. Marmorstein AD, Johnson AA, Bachman LA et al (2018) Mutant Best1 expression and impaired phagocytosis in an iPSC model of autosomal recessive bestrophinopathy. Sci Rep 8:4487. https://doi.org/10.1038/s41598-018-21651-z
74. Li Y, Zhang Y, Xu Y et al (2017) Patient-specific mutations impair BESTROPHIN1's essential role in mediating Ca^{2+}-dependent Cl^- currents in human RPE. Elife 6:e29914. https://doi.org/10.7554/eLife.29914
75. Moshfegh Y, Velez G, Li Y, Bassuk AG, Mahajan VB, Tsang SH (2016) BESTROPHIN1 mutations cause defective chloride conductance in patient stem cell-derived RPE. Hum Mol Genet 25:2672–2680. https://doi.org/10.1093/hmg/ddw126
76. Zhao Q, Kong Y, Kittredge A et al (2021) Distinct expression requirements and rescue strategies for *BEST1* loss- and gain-of-function mutations. Elife 10:e67622. https://doi.org/10.7554/eLife.67622
77. Guziewicz KE, McTish E, Dufour VL et al (2018) Underdeveloped RPE apical domain underlies lesion formation in canine bestrophinopathies. Adv Exp Med Biol 1074:309–315. https://doi.org/10.1007/978-3-319-75402-4_38
78. Zhuk SA, Edwards AO (2006) Peripherin/RDS and VMD2 mutations in macular dystrophies with adult-onset vitelliform lesion. Mol Vis 12:811–815
79. Bianco L, Arrigo A, Antropoli A et al (2023) *PRPH2*-Associated retinopathy: Novel variants and genotype-phenotype correlations. Ophthalmol Retina 7:450–461. https://doi.org/10.1016/j.oret.2022.12.008
80. Rosenthal R, Bakall B, Kinnick T et al (2006) Expression of bestrophin-1, the product of the *VMD2* gene, modulates voltage-dependent Ca^{2+} channels in retinal pigment epithelial cells. FASEB J 20:178–180. https://doi.org/10.1096/fj.05-4495fje
81. Neussert R, Müller C, Milenkovic VM, Strauss O (2010) The presence of bestrophin-1 modulates the Ca^{2+} recruitment from Ca^{2+} stores in the ER. Pflugers Arch 460:163–175. https://doi.org/10.1007/s00424-010-0840-2
82. Arora R, Khan K, Kasilian ML et al (2016) Unilateral *BEST1*-associated retinopathy. Am J Ophthalmol 169:24–32. https://doi.org/10.1016/j.ajo.2016.05.024
83. Bianco L, Arrigo A, Antropoli A et al (2024) Multimodal imaging in best vitelliform macular dystrophy: literature review and novel insights. Eur J Ophthalmol 34:39–51. https://doi.org/10.1177/11206721231166434
84. Ratra D, Karra A (2025) Unilateral best vitelliform macular dystrophy- a case series. Doc Ophthalmol 150:111–116. https://doi.org/10.1007/s10633-025-10008-3
85. Tatemoto Y, Hayashi T, Mizobuchi K, Den S, Nakano T (2025) Best vitelliform macular dystrophy caused by a BEST1 p.(Ser246Asn) variant coexisting with diabetic retinopathy. Doc Ophthalmol. https://doi.org/10.1007/s10633-025-10056-9
86. Kumar V, Chatra K (2018) Fibrotic pillar leads to focal choroidal excavation in best vitelliform dystrophy. Graefes Arch Clin Exp Ophthalmol 256:2083–2087. https://doi.org/10.1007/s00417-018-4120-8
87. Nourinia R, Roshandel D, Lima BS, Sayanjali S (2015) Best disease associated with macular hole. Retin Cases Brief Rep 9:7–12. https://doi.org/10.1097/ICB.0000000000000068
88. Pozzoni MC, Fine HF, Ferrara DC, Klancnik JM Jr, Engelbert M, Yannuzzi LA (2012) Peripapillary choroidal neovascularization in best disease. Retin Cases Brief Rep 6:176–178. https://doi.org/10.1097/ICB.0b013e318223d24ds
89. Querques G, Regenbogen M, Quijano C, Delphin N, Soubrane G, Souied EH (2008) High-definition optical coherence tomography features in vitelliform macular dystrophy. Am J Ophthalmol 146:501–507. https://doi.org/10.1016/j.ajo.2008.05.029
90. Schatz P, Sharon D, Al-Hamdani S, Andréasson S, Larsen M (2016) Retinal structure in young patients aged 10 years or less with best vitelliform macular dystrophy. Graefes Arch Clin Exp Ophthalmol 254:215–221. https://doi.org/10.1007/s00417-015-3025-z
91. Querques G, Zerbib J, Santacroce R et al (2011) The spectrum of subclinical best vitelliform macular dystrophy in subjects with mutations in *BEST1* gene. Invest Ophthalmol Vis Sci 52:4678–4684. https://doi.org/10.1167/iovs.10-6500
92. Sparrow JR, Duncker T, Woods R, Delori FC (2016) Quantitative fundus autofluorescence in best vitelliform macular dystrophy: RPE lipofuscin is not increased in non-lesion areas of retina. Adv Exp Med Biol 854:285–290. https://doi.org/10.1007/978-3-319-17121-0_38
93. Bakall B, Radu RA, Stanton JB et al (2007) Enhanced accumulation of A2E in individuals homozygous or heterozygous for mutations in *BEST1 (VMD2)*. Exp Eye Res 85:34–43. https://doi.org/10.1016/j.exer.2007.02.018
94. Maia-Lopes S, Silva ED, Reis A, Silva MF, Mateus C, Castelo-Branco M (2008) Retinal function in best macular dystrophy: relationship between electrophysiological, psychophysical, and structural measures of damage. Invest Ophthalmol Vis Sci 49:5553–5560. https://doi.org/10.1167/iovs.08-2093
95. Kay CN, Abramoff MD, Mullins RF et al (2012) Three-dimensional distribution of the vitelliform lesion, photoreceptors, and retinal pigment epithelium in the macula of patients with best vitelliform macular dystrophy. Arch Ophthalmol 130:357–364. https://doi.org/10.1001/archophthalmol.2011.363
96. de Carvalho JR, Paavo M, Chen L, Chiang J, Tsang SH, Sparrow JR (2019) Multimodal imaging in best vitelliform macular dystrophy. Invest Ophthalmol Vis Sci 60:2012–2022. https://doi.org/10.1167/iovs.19-26571

97. Liu J, Xuan Y, Zhang Y, Liu W, Xu G (2017) Bilateral macular holes and a new onset vitelliform lesion in best disease. Ophthalmic Genet 38:79–82. https://doi.org/10.3109/13816810.2015.1126614
98. Parodi MB, Zucchiatti I, Fasce F, Bandello F (2014) Bilateral choroidal excavation in best vitelliform macular dystrophy. Ophthalmic Surg Lasers Imaging Retina 45:e8–e10. https://doi.org/10.3928/23258160-20140205-01
99. Low S, Davidson AE, Holder GE et al (2011) Autosomal dominant Best disease with an unusual electrooculographic light rise and risk of angle-closure glaucoma: a clinical and molecular genetic study. Mol Vis 2011:2272–2282
100. Gupta V, Chawla R, Kumar V (2024) Bull's-eye maculopathy in best vitelliform dystrophy. Ophthalmol Retina 8:e51. https://doi.org/10.1016/j.oret.2024.05.007
101. Singuri S, DeBenedictis MJ, Traboulsi EI, Yuan A, Schur RM (2025) *BEST1* variant associated with an atypical macular and peripheral retinal phenotype. Retin Cases Brief Rep 19:129–134. https://doi.org/10.1097/ICB.0000000000001520
102. Toto L, Boon CJ, Antonio D et al (2016) Bestrophinopathy: a spectrum of ocular abnormalities caused by the c.614T>C mutation in the *BEST1* gene. Retina 36:1586–1595. https://doi.org/10.1097/IAE.0000000000000950
103. Wong RL, Hou P, Choy KW et al (2010) Novel and homozygous *BEST1* mutations in Chinese patients with Best vitelliform macular dystrophy. Retina 30:820–827. https://doi.org/10.1097/IAE.0b013e3181c700c1
104. Duncker T, Greenberg JP, Ramachandran R et al (2014) Quantitative fundus autofluorescence and optical coherence tomography in Best vitelliform macular dystrophy. Invest Ophthalmol Vis Sci 55:1471–1482. https://doi.org/10.1167/iovs.13-13834
105. Theischen M, Schilling H, Steinhorst UH (1997) EOG in adult vitelliform macular degeneration, butterfly-shaped pattern dystrophy and Best disease. Ophthalmologe 94:230–233. https://doi.org/10.1007/s003470050107
106. Jarc-Vidmar M, Popović P, Hawlina M, Brecelj J (2001) Pattern ERG and psychophysical functions in best's disease. Doc Ophthalmol 103:47–61. https://doi.org/10.1023/a:1017963015883
107. Polosa A, Lu M, Dorfman AL, Masis-Solano M, Costantino S, Qian CX (2025) Characterization of functional and structural impairments in Best vitelliform macular dystrophy using visual electrophysiology and optical coherence tomography in pediatric and adult patients. Doc Ophthalmol. https://doi.org/10.1007/s10633-025-10064-9
108. Power WJ, Coleman K, Curtin DM, Mooney DJ (1990) The pattern ERG in Best's disease. Doc Ophthalmol 76:279–284. https://doi.org/10.1007/BF00142687
109. Kaufman SJ, Goldberg MF, Orth DH, Fishman GA, Tessler H, Mizuno K (1982) Autosomal dominant vitreoretinochoroidopathy. Arch Ophthalmol 100:272–278. https://doi.org/10.1001/archopht.1982.01030030274008
110. Mainguy A, Dhaenens CM, Poncet A et al (2024) Variable expressivity of the autosomal dominant vitreoretinochoroidopathy (ADVIRC) phenotype associated with a novel variant in *BEST1*. Ophthalmic Genet 45:470–475. https://doi.org/10.1080/13816810.2024.2368797
111. Vincent A, McAlister C, Vandenhoven C, Héon E (2011) BEST1-related autosomal dominant vitreoretinochoroidopathy: a degenerative disease with a range of developmental ocular anomalies. Eye 25:113–118. https://doi.org/10.1038/eye.2010.165
112. Wöster L, Roider J (2018) Long-term changes in autosomal dominant vitreoretinochoroidopathy (ADVIRC). Graefes Arch Clin Exp Ophthalmol 256:441–442. https://doi.org/10.1007/s00417-017-3810-y
113. Traboulsi EI, Payne JW (1993) Autosomal dominant vitreoretinochoroidopathy. Report of the third family. Arch Ophthalmol 111:194–196. https://doi.org/10.1001/archopht.1993.01090020048021
114. White K, Marquardt A, Weber BH (2000) *VMD2* mutations in vitelliform macular dystrophy (best disease) and other maculopathies. Hum Mutat 15:301–308. https://doi.org/10.1002/(SICI)1098-1004(200004)15:4%3c301::AID-HUMU1%3e3.0.CO;2-N
115. Tekin K, Dulger SC, Horozoglu Ceran T, Inanc M, Ozdal PC, Teke MY (2024) Multimodal imaging and genetic characteristics of autosomal recessive bestrophinopathy. J Fr Ophtalmol 47:104097. https://doi.org/10.1016/j.jfo.2024.104097
116. Miura M, Makita S, Yasuno Y et al (2024) Multimodal imaging analysis of autosomal recessive bestrophinopathy: case series. Medicine 103:e38853. https://doi.org/10.1097/MD.0000000000038853
117. Burgess R, Millar ID, Leroy BP et al (2008) Biallelic mutation of *BEST1* causes a distinct retinopathy in humans. Am J Hum Genet 82:19–31. https://doi.org/10.1016/j.ajhg.2007.08.004
118. Khojasteh H, Azarmina M, Ebrahimiadib N et al (2021) Autosomal recessive bestrophinopathy: clinical and genetic characteristics of twenty-four cases. J Ophthalmol 2021:6674290. https://doi.org/10.1155/2021/6674290
119. Casalino G, Khan KN, Armengol M et al (2021) Autosomal recessive bestrophinopathy: clinical features, natural history, and genetic findings in preparation for clinical trials. Ophthalmology 128:706–718. https://doi.org/10.1016/j.ophtha.2020.10.006
120. Li JX, Meng LR, Hou BK et al (2024) Detection of novel *BEST1* variations in autosomal recessive bestrophinopathy using third-generation sequencing. Curr Med Sci 44:419–425. https://doi.org/10.1007/s11596-024-2865-3
121. Lee CS, Jun I, Choi SI et al (2015) A novel *BEST1* mutation in autosomal recessive bestrophinopathy. Invest Ophthalmol Vis Sci 56:8141–8150. https://doi.org/10.1167/iovs.15-18168
122. Pomares E, Burés-Jelstrup A, Ruiz-Nogales S, Corcóstegui B, González-Duarte R, Navarro R (2012) Nonsense-mediated decay as the molecular cause for autosomal recessive bestrophinopathy in two unrelated families. Invest Ophthalmol Vis Sci 53:532–537. https://doi.org/10.1167/iovs.11-7964
123. Johnson AA, Bachman LA, Gilles BJ et al (2015) Autosomal recessive bestrophinopathy is not associated with the loss of bestrophin-1 anion channel function in a patient with a novel *BEST1* mutation. Invest Ophthalmol

Vis Sci 56:4619–4630. https://doi.org/10.1167/iovs.15-16910
124. Renner AB, Tillack H, Kraus H et al (2004) Morphology and functional characteristics in adult vitelliform macular dystrophy. Retina 24:929–939. https://doi.org/10.1097/00006982-200412000-00014
125. Nipp GE, Lee T, Sarici K, Malek G, Hadziahmetovic M (2023) Adult-onset foveomacular vitelliform dystrophy: epidemiology, pathophysiology, imaging, and prognosis. Front Ophthalmol 3:1237788. https://doi.org/10.3389/fopht.2023.1237788
126. Tiosano L, Grunin M, Hagbi-Levi S, Banin E, Averbukh E, Chowers I (2016) Characterising the phenotype and progression of sporadic adult-onset foveomacular vitelliform dystrophy. Br J Ophthalmol 100:1476–1481. https://doi.org/10.1136/bjophthalmol-2015-307658
127. Querques G, Forte R, Querques L, Massamba N, Souied EH (2011) Natural course of adult-onset foveomacular vitelliform dystrophy: a spectral-domain optical coherence tomography analysis. Am J Ophthalmol 152:304–313. https://doi.org/10.1016/j.ajo.2011.01.047
128. Jaffe GJ, Schatz H (1988) Histopathologic features of adult-onset foveomacular pigment epithelial dystrophy. Arch Ophthalmol 106:958–960. https://doi.org/10.1001/archopht.1988.01060140104034
129. Patrinely JR, Lewis RA, Font RL (1985) Foveomacular vitelliform dystrophy, adult type. A clinicopathologic study including electron microscopic observations. Ophthalmology 92:1712–1718. https://doi.org/10.1016/s0161-6420(85)34097-6
130. Arnold JJ, Sarks JP, Killingsworth MC, Kettle EK, Sarks SH (2003) Adult vitelliform macular degeneration: a clinicopathological study. Eye 17:717–726. https://doi.org/10.1038/sj.eye.6700460
131. Dubovy SR, Hairston RJ, Schatz H et al (2000) Adult-onset foveomacular pigment epithelial dystrophy: clinicopathologic correlation of three cases. Retina 20:638–649
132. Saito W, Yamamoto S, Hayashi M, Ogata K (2003) Morphological and functional analyses of adult onset vitelliform macular dystrophy. Br J Ophthalmol 87:758–762. https://doi.org/10.1136/bjo.87.6.758
133. Brar AS, Parameswarappa DC, Takkar B et al (2024) Gene therapy for inherited retinal diseases: from laboratory bench to patient bedside and beyond. Ophthalmol Ther 13:21–50. https://doi.org/10.1007/s40123-023-00862-2
134. Guziewicz KE, Zangerl B, Lindauer SJ et al (2007) Bestrophin gene mutations cause canine multifocal retinopathy: a novel animal model for best disease. Invest Ophthalmol Vis Sci 48:1959–1967. https://doi.org/10.1167/iovs.06-1374
135. Guziewicz KE, Cideciyan AV, Beltran WA et al (2018) *BEST1* gene therapy corrects a diffuse retina-wide microdetachment modulated by light exposure. Proc Natl Acad Sci U S A 115:E2839–E2848. https://doi.org/10.1073/pnas.1720662115
136. Marmorstein LY, Wu J, McLaughlin P et al (2006) The light peak of the electroretinogram is dependent on voltage-gated calcium channels and antagonized by bestrophin (best-1). J Gen Physiol 127:577–589. https://doi.org/10.1085/jgp.200509473
137. Zhang Y, Stanton JB, Wu J et al (2010) Suppression of Ca^{2+} signaling in a mouse model of best disease. Hum Mol Genet 19:1108–1118. https://doi.org/10.1093/hmg/ddp583
138. Yi W, Xu M, Xue Y et al (2025) A spontaneous nonhuman primate model of inherited retinal degeneration. JCI Insight 10:e190807. https://doi.org/10.1172/jci.insight.190807
139. Sinha D, Steyer B, Shahi PK et al (2020) Human iPSC modeling reveals mutation-specific responses to gene therapy in a genotypically diverse dominant maculopathy. Am J Hum Genet 107:278–292. https://doi.org/10.1016/j.ajhg.2020.06.011
140. Singh R, Kuai D, Guziewicz KE et al (2015) Pharmacological modulation of photoreceptor outer segment degradation in a human iPS cell model of inherited macular degeneration. Mol Ther 23:1700–1711. https://doi.org/10.1038/mt.2015.141
141. Arden GB, Barrada A, Kelsey JH (1962) New clinical test of retinal function based upon the standing potential of the eye. Br J Ophthalmol 46:449–467. https://doi.org/10.1136/bjo.46.8.449
142. Lessel MR, Thaler A, Scheiber V, Heilig P (1993) The dark trough in clinical electro-oculography. Influence of preadaptation on amplitudes and latencies. Doc Ophthalmol 84:31–38. https://doi.org/10.1007/BF01203280
143. Arden GB, Kelsey JH (1962) Some observations on the relationship between the standing potential of the human eye and the bleaching and regeneration of visual purple. J Physiol 161:205–226. https://doi.org/10.1113/jphysiol.1962.sp006882
144. Marmor MF, Zrenner E (1993) Standard for clinical electro-oculography. International Society for Clinical Electrophysiology of Vision. Arch Ophthalmol 111:601–604. https://doi.org/10.1001/archopht.1993.01090050035023
145. Miles WR (1939) Experimental modification of the polarity potential of the human eye. Yale J Biol Med 12:161–183
146. Griff ER, Steinberg RH (1982) Origin of the light peak: in vitro study of *Gekko gekko*. J Physiol 331:637–652. https://doi.org/10.1113/jphysiol.1982.sp014395
147. Constable PA, Ngo D, Quinn S, Thompson DA (2017) A meta-analysis of clinical electro-oculography values. Doc Ophthalmol 135:219–232. https://doi.org/10.1007/s10633-017-9616-8
148. van Norren D, Heynen H (1986) Origin of the fast oscillation in the electroretinogram of the macaque. Vision Res 26:569–575. https://doi.org/10.1016/0042-6989(86)90005-2
149. Linsenmeier RA, Steinberg RH (1984) Delayed basal hyperpolarization of cat retinal pigment epithelium and its relation to the fast oscillation of the DC electroretinogram. J Gen Physiol 83:213–232. https://doi.org/10.1085/jgp.83.2.213
150. Griff ER, Steinberg RH (1984) Changes in apical $[K^+]$ produce delayed basal membrane responses of the retinal pigment epithelium in the gecko. J Gen Physiol 83:193–211. https://doi.org/10.1085/jgp.83.2.193

151. Gallemore RP, Hernandez E, Tayyanipour R, Fujii S, Steinberg RH (1993) Basolateral membrane Cl^- and K^+ conductances of the dark-adapted chick retinal pigment epithelium. J Neurophysiol 70:1656–1668. https://doi.org/10.1152/jn.1993.70.4.1656
152. Fortenbach C, Peinado Allina G, Shores CM et al (2021) Loss of the K^+ channel $K_v2.1$ greatly reduces outward dark current and causes ionic dysregulation and degeneration in rod photoreceptors. J Gen Physiol 153:e202012687. https://doi.org/10.1085/jgp.202012687
153. Hagins WA, Penn RD, Yoshikami S (1970) Dark current and photocurrent in retinal rods. Biophys J 10(5):380–412. https://doi.org/10.1016/S0006-3495(70)86308-1
154. Bialek S, Joseph DP, Miller SS (1995) The delayed basolateral membrane hyperpolarization of the bovine retinal pigment epithelium: mechanism of generation. J Physiol 484(Pt 1):53–67. https://doi.org/10.1113/jphysiol.1995.sp020647
155. Schneck ME, Fortune B, Adams AJ (2000) The fast oscillation of the electrooculogram reveals sensitivity of the human outer retina/retinal pigment epithelium to glucose level. Vision Res 40:3447–3453. https://doi.org/10.1016/s0042-6989(00)00173-5
156. Schneck ME, Shupenko L, Adams AJ (2008) The fast oscillation of the EOG in diabetes with and without mild retinopathy. Doc Ophthalmol 116:231–236. https://doi.org/10.1007/s10633-007-9088-3
157. Weleber RG (1989) Fast and slow oscillations of the electro-oculogram in best's macular dystrophy and retinitis pigmentosa. Arch Ophthalmol 107:530–537. https://doi.org/10.1001/archopht.1989.01070010544028
158. Mergaerts F, Daems E, Van Malderen L, Spileers W (2001) Recording of the fast oscillations in the human electro-oculogram. Doc Ophthalmol 103:63–72. https://doi.org/10.1023/a:1017915132721
159. Padhy SK, Constable PA (2026) The short wavelength electro-oculogram (SW-EOG) in best disease: preliminary results. Doc Ophthalmol. https://doi.org/10.1007/s10633-026-10081-2
160. Constable PA, Kapoor G (2021) Is white the right light for the clinical electrooculogram? Doc Ophthalmol 143:297–304. https://doi.org/10.1007/s10633-021-09845-9
161. Hamilton R (2021) Clinical electrophysiology of vision-commentary on current status and future prospects. Eye 35:2341–2343. https://doi.org/10.1038/s41433-021-01592-0